Seismic data with different bandwidths: An example from Catcher East, North Sea

Bo Zhao, Truman Holcombe, Howard Rael, and Alan Cohen, ION GX Technology*

Summary

In recent years, both acquisition and processing technologies have been utilized to broaden seismic data bandwidth. Although there has been some confusion in understanding the processing only techniques, there have also been successful applications. This paper analyzes seismic data processed using broadband technologies from three aspects: spectrum normalization, signal-to-noise, and seismic inversion. The results show that broadband processing technology can enhance both low and high frequencies, boost the signal-to-noise ratios, and improve seismic inversions, and that robust quantitative interpretation of broadband seismic data may lead to better business decisions.

Introduction

We applied the WiBand^{TM} technique to shallow-tow and deep-tow seismic data from Catcher East in the North Sea. WiBand is an effective broadband processing method that employs a new de-ghosting technique to remove most of the ghost effects from conventional streamer data (Zhou et al., 2012). The original and WiBand shallow-tow seismic data are demonstrated in Figures 1 and 2, respectively.

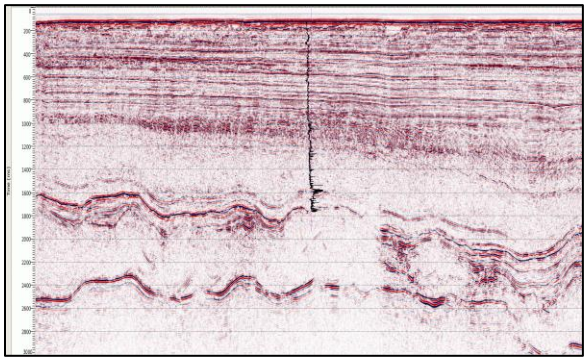

Figure 1. *The original shallow-tow seismic data profile. The inserted well log curve is P-wave impedance.*

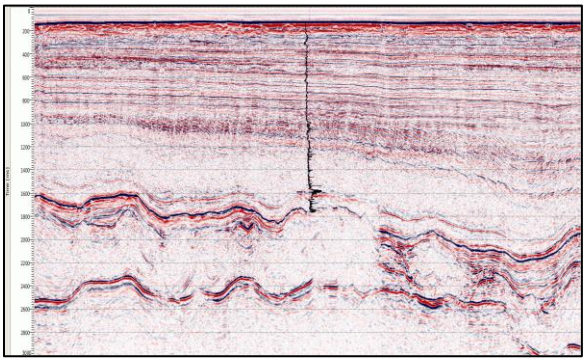

Figure 2. *The shallow-tow seismic data after WiBand is applied.*

Figure 3 shows the spectra of the original shallow-tow and the WiBand data, which have been normalized with respect to the peak spectral amplitude. It appears that the normalized spectrum of the WiBand data has more low frequencies and less high frequencies than the normalized spectrum of the original shallow-tow data. This is contrary to what we often observe which is that WiBand seismic data has both low and high frequencies. As shown in Figure 3, the WiBand data spectrum has a slightly wider bandwidth at -3 dB than the original seismic data. Evidently, the bandwidth of WiBand data is much wider than the bandwidth of the original seismic below -5 dB. This suggests that normalizing the seismic spectra of different bandwidths with respect to the peak spectral amplitude could result in a complicated picture.

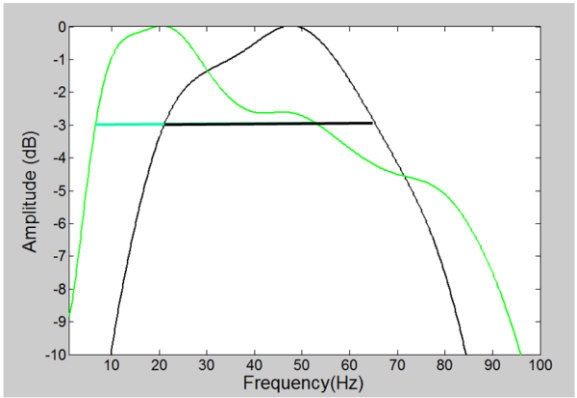

Figure 3. *Spectral normalization of original seismic (black) and WiBand seismic (green) data.*

DOI http://dx.doi.org/10.1190/segam2014-0198.1

Seismic data with different bandwidths

In the following, we discuss normalizing the spectra with a spectral model, then analyzing the seismic data of different bandwidths from three aspects: spectra comparison, signal-to-noise ratio, and seismic inversion.

Normalize Spectra with a Spectral Model:

Dolan and Bean (1997) modeled the power spectrum of three super-deep borehole wire-line logs in wavenumber domain as $k^{-\beta}$ (where k = wavenumber and exponent $\beta = 5 - 2D$, for fractal dimension D). Fractal dimension is a ratio comparing how the detail in a pattern changes with the scale in describing self-similarity (Mandelbrot, 1977). In the frequency domain, the power spectrum can be modeled as $f^{-(5-2D)}$ with only one variable of fractal dimension D. For D = 2, the model becomes *1/f*, a special case of the spectral model with fractal dimension.

Figure 4 shows the comparison of an average log spectrum, the curve of a constant fractal dimension (blue, D = 1.85), and spectral model of 1/f (red). The average log spectra of 15 impedance logs are plotted as the dotted black line. Between 10 Hz and 100 Hz, the spectral models fit the average log spectrum reasonably well. Below 10 Hz, the spectral models have a lower amplitude than the average log spectrum, and the model with a fractal dimension less than 2 (blue) is closer to the average log spectrum than the model of 1/*f* (red).

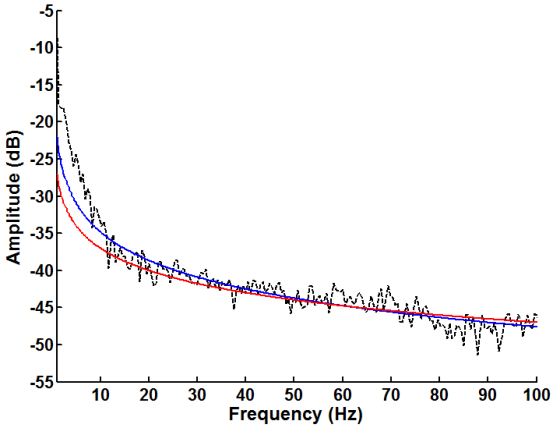

Figure 4. *Average log spectrum from the relevant wells (dotted black line), spectral model with a fractal dimension of 1.85 (blue), and spectral model of 1/f (red).*

We extracted four seismic wavelets from a line in the Catcher East dataset and compared the spectra of the seismic data with different bandwidths (Figure 5). The spectra are normalized to the peak spectral amplitude in the lower panel. The spectra of the WiBand data appear to have more low and fewer high frequencies than the spectra of the original data. The analysis window is 1-2 s and includes all the traces from the four different datasets. Compared to the shallow-tow original dataset, the deep-tow original dataset has more low frequencies but it shows a ghost notch around 48Hz.

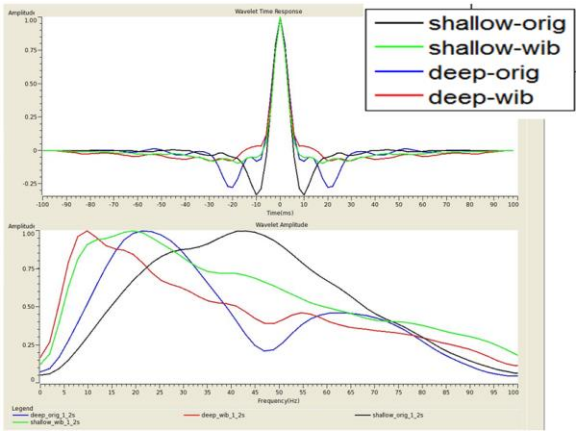

Figure 5. *Seismic wavelets and spectra normalized to the peak spectral amplitude: shallow-tow original (black), shallow-tow WiBand (green), deep-tow original (blue), and deep-tow WiBand (red).*

However, if the estimated spectra of the original and WiBand seismic data are normalized along a spectral model matching the average log spectrum, the spectrum after WiBand has richer frequency contents in both the low and high frequencies (Figure 6).

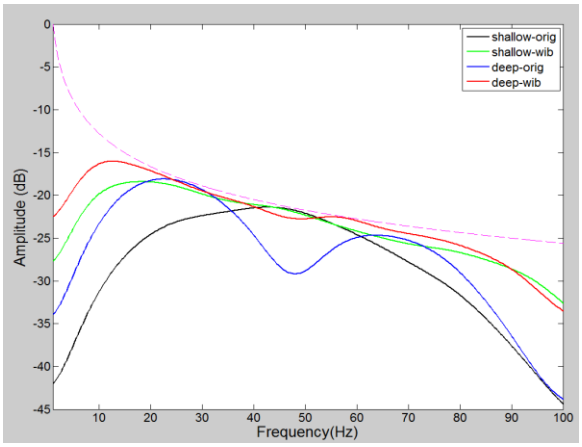

Figure 6. *Spectra normalized to a spectral model matching the average log spectrum (magenta dashed line): shallow-tow original (black), shallow-tow WiBand (green), deep-tow original (blue), and deep-tow WiBand (red).*

Signal and Noise Analysis:

Signal and noise analysis is another effective way to compare the seismic data with different bandwidths. Figure 7 compares the signal and noise spectra of the shallow-tow data before and after WiBand processing. The signal and noise spectra were estimated using the White (1984) method.

DOI http://dx.doi.org/10.1190/segam2014-0198.1

Seismic data with different bandwidths

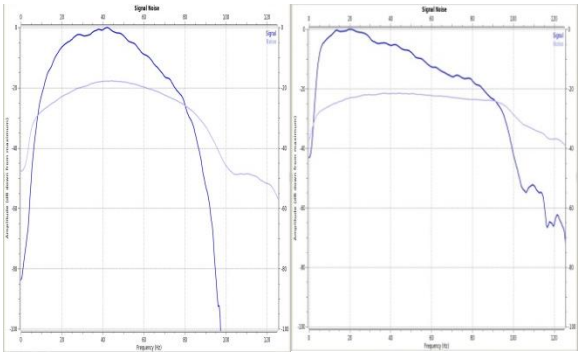

Figure 7. *The signal (dark blue) and noise (light blue) spectra of the shallow-tow data before (left) and after (right) WiBand processing.*

The signal-to-noise (S/N) ratios before and after WiBand processing are plotted in Figure 8. The S/N ratio after WiBand processing (blue) is higher than the S/N ratio before WiBand at both the low and high frequencies.

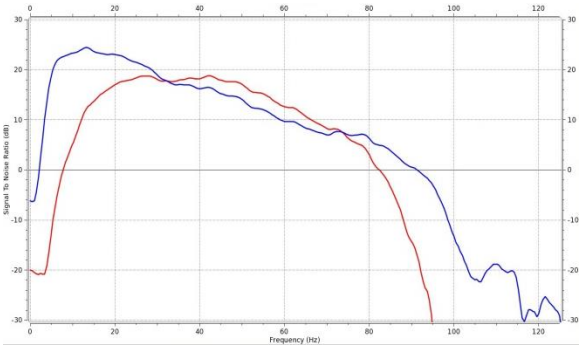

Figure 8*. The S/N ratios before (red) and after (blue) WiBand processing.*

Overlaying the S/N ratio on the seismic data section is another way of comparing the differences before and after WiBand processing. Figure 9 shows the colored S/N ratio overlay on the original shallow-tow data. As demonstrated, the S/N ranges around 8-11 dB (the green color zone) at the 1500-1900 ms time window, which is higher than the rest of the section. For S/N estimation (from auto- and cross-power spectra), a window of 50 traces by 100 samples was used.

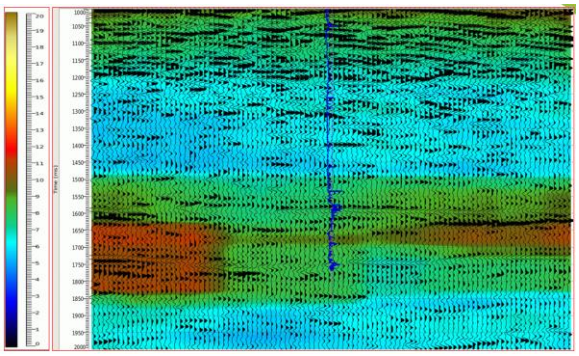

Figure 9. *Shallow-tow original data overlaid with the S/N ratio.*

The overlay of colored S/N ratio on the shallow-tow WiBand data is shown in Figure 10. For the same time window of 1500-1900 ms, the WiBand data shows an even higher S/N ratio (around 9-13 dB) compared to the S/N ratio of the original data (Figure 9).

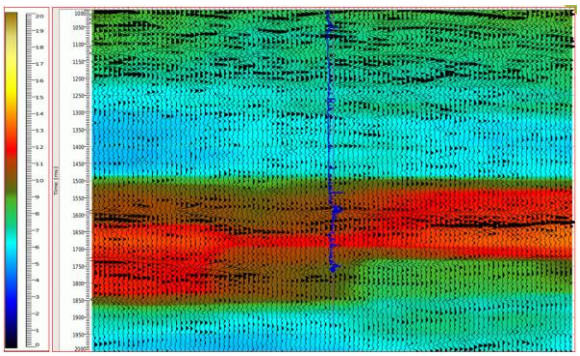

Figure 10. *Shallow-tow WiBand data overlaid with the S/N ratio.*

Inversion Results:

The model-based post-stack inversions were performed separately on the original and WiBand datasets. The low frequency model was built from available well logs and seismic data between two interpreted horizons at 800 ms and 1700 ms at the well location. The wavelets were estimated individually from the original and WiBand data, and then were used in separate correlations with the well logs and different seismic volumes. After building the low frequency model and estimating the wavelets, acoustic impedance volumes were inverted from both the original and WiBand data.

As illustrated in Figure 12, the inverted impedance from the WiBand data is more continuous laterally and better matches the well log compared to the inverted impedance from the original data (Figure 11).

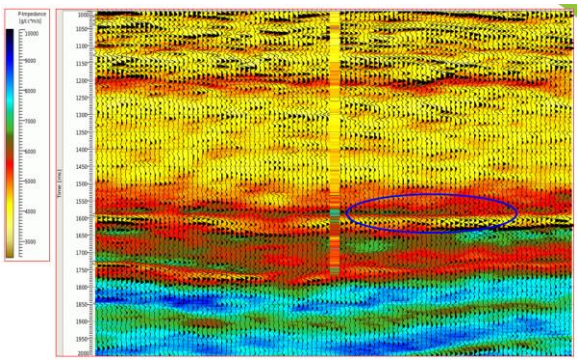

Figure 11. *Impedance profile from the P-wave post-stack inversion of the shallow-tow original data. The inserted column is the impedance log.*

DOI http://dx.doi.org/10.1190/segam2014-0198.1

Seismic data with different bandwidths

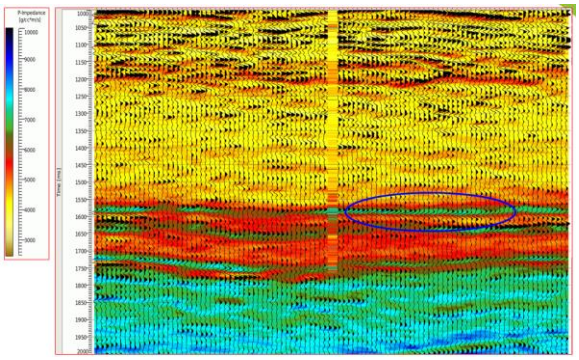

Figure 12. *Impedance profile from the P-wave post-stack inversion of the shallow-tow data with WiBand. The inserted column is the impedance log.*

Conclusions:

This paper analyzes seismic data with different bandwidths from three aspects: spectrum normalization, signal-to-noise, and seismic inversion. Our analysis shows that if the spectra of seismic data before and after WiBand are normalized along a spectral model, which could match the average log spectrum, the spectrum after WiBand has richer frequency content both in the low and high frequencies. The signal-to-noise ratio analysis demonstrates that seismic data processed with WiBand has higher signal-to-noise ratios for both low and high frequencies. Finally, the inversion comparison shows the inverted impedance from WiBand data is more continuous laterally and matches the well log better than the impedance from the original data. This paper concludes that ultimately, robust quantitative interpretation of broadband seismic data may lead to better business decisions.

Acknowledgements:

We thank Yanrong Hu, Tiancong Hong, and Farshid Forouhideh for their constructive discussions and suggestions. We thank Reda Meftahi, Dave King, and Artur Tatarata for the WiBand processing. We appreciate management support from ION GX Technology and Polarcus in publishing the results of this case study.

DOI http://dx.doi.org/10.1190/segam2014-0198.1

http://dx.doi.org/10.1190/segam2014-0198.1

EDITED REFERENCES

Note: This reference list is a copy-edited version of the reference list submitted by the author. Reference lists for the 2014 SEG Technical Program Expanded Abstracts have been copy edited so that references provided with the online metadata for each paper will achieve a high degree of linking to cited sources that appear on the Web.

REFERENCES

Dolan, S. S., and C. J. Bean, 1997, Some remarks on the estimation of fractal scaling parameters from borehole wire-line logs: Geophysical Research Letters, **24**, no. 10, 1271–1274, http://dx.doi.org/10.1029/97GL00987.

Mandelbrot, B., 1977, Fractals: Form, chance and dimension: W. H. Freeman.

White, R. E., 1984, Signal and noise estimation from seismic reflection data using spectral coherence methods: Proceedings of the IEEE, **72**, no. 10, 1340–1356, http://dx.doi.org/10.1109/PROC.1984.13022.

Zhou, Z., M. Cvetkovic, B. Xu, and P. Fontana, 2012, Analysis of a broadband processing technology applicable to conventional streamer data: First Break, **30**, no. 10, 77–84.

DOI http://dx.doi.org/10.1190/segam2014-0198.1